Effective suppressibility of chaos

Álvaro G. López, Jesús M. Seoane, and Miguel A. F. Sanjuán
Departamento de Física, Nonlinear Dynamics, Chaos and Complex Systems Group,
Universidad Rey Juan Carlos, Tulipán s/n, 28933 Móstoles, Madrid, Spain

Suppression of chaos is a relevant phenomenon that can take place in nonlinear dynamical systems when a parameter is varied. Here, we investigate the possibilities of effectively suppressing the chaotic motion of a dynamical system by a specific time independent variation of a parameter of our system. In realistic situations, we need to be very careful with the experimental conditions and the accuracy of the parameter measurements. We define the suppressibility, a new measure taking values in the parameter space, that allows us to detect which chaotic motions can be suppressed, what possible new choices of the parameter guarantee their suppression, and how small the parameter variations from the initial chaotic state to the final periodic one are. We apply this measure to a Duffing oscillator and a system consisting on ten globally coupled Hénon maps. We offer as our main result tool sets that can be used as guides to suppress chaotic dynamics. © 2013 AIP Publishing LLC. [http://dx.doi.org/10.1063/1.4803521]

Chaotic dynamical systems present sensitivity to initial conditions, what makes their evolution to become unpredictable for long enough times. Nonetheless, in many situations, we need to deal with systems displaying predictable behavior. A possible way to suppress chaos is by adding suitable small perturbations to a system, which typically depend on one or more parameters. If we have a thorough knowledge of the precision in the measurement of these parameters and the response of the system to their variations, we can use them to improve the predictability. This task can be performed with the help of the *chaotic parameter set*, which in parameter space informs us about the periodicity of a certain dynamical system. Our main goal is to quantify the possibilities that a system offers to make transitions from a chaotic regime to a regular one under some given conditions. For that purpose, we introduce a new concept, defined by means of the chaotic parameter set, that we call *suppressibility*. The suppressibility tells us for which regions in the parameter space the dynamics of a system can be more easily and in more ways suppressed. We also present two different sets that can be used as guides to suppress chaotic dynamics by the variation of a parameter: the *suppression parameter set* and the *set of the total accessible transitions*. The suppressibility measure is numerically tested for both, a flow and a discrete dynamical system, showing the generality of this technique.

I. INTRODUCTION

Sometimes chaotic dynamics represents an advantage because it makes systems more adaptable. However, in other situations, it is an undesirable effect. As a consequence, it restricts the operating range of many electronic and mechanic devices. This is a good enough reason to justify the attention that *chaos suppression* has received in the study of dynamical systems.[1–4] In the case of nonlinear oscillators, such a suppression can be accomplished by introducing a

time periodic perturbation depending on a set of predetermined parameters, which can be chosen to cause an stabilization of the chaotic system toward a periodic state. Contrary to some *feedback* control methods, as for example, the celebrated OGY,[5] in which state dependent parameter perturbations are performed to stabilize an unstable periodic orbit, the present case is of the essence of some *nonfeedback* control methods, as for example, the phase control.[6] In the phase control method, typically time independent variations of a phase difference between the periodic perturbations acting on a certain nonlinear oscillator is used to achieve chaos suppression. Sometimes anharmonic periodic perturbations have been used, as it is the case of Jacobi elliptic functions,[3,7] for which the elliptic parameter has been selected as the control parameter. Whatever the perturbation is, it always depends on one or more parameters, so studying the response of the dynamical behavior for the perturbed system to their variations is required. This task can be managed analytically or numerically. In the former case, one of the commonly used methods is the Melnikov analysis,[3] while in the last one bifurcation diagrams or chaotic parameter sets are computed.[7,8] Just to recall a chaotic parameter set informs us if the asymptotic dynamics of a system is chaotic or not when varying two system parameters. The fact that it involves two parameters makes this set specially useful, what explains its frequent use in the study of chaos suppression.[4,7–10] The usefulness of these theoretical results is that they might be later used in experimental settings[11] as guides to suppress chaotic dynamics. Nevertheless, in experimental situations, parameters are measured with a finite accuracy. This means that a certain parameter variation, appearing in a bifurcation diagram as adequate, could be uneffective in practice due to the limited precision with which such a parameter is measured. The main goal of this paper is to study when it is in practice possible to turn the asymptotic dynamics of a system from chaotic to periodic by variations of a parameter. Having settled a domain for that parameter, we want to know if suppression is in fact feasible for many different values spread

over it, and if it is carried out with small variations of the parameter or not. For such purpose, we define the *suppressibility*, a measure that takes into account all these matters. Sometimes it occurs that chaotic parameter sets exhibit highly fractal patterns. In those situations, we have no security of reaching one asymptotic behavior or the opposite, due to the limited precision with which we measure a parameter. For this reason, we have to provide a way to not consider them when defining and studying effective suppression. As we will see, our numerical study can be carried out in the parameter space by means of the chaotic parameter set.

The paper is organized as follows. In Sec. II, a brief description of the used model to illustrate our study is given. In Sec. III, the chaotic parameter set is introduced. Later on, in Sec. IV, we define the suppressibility, a measure that calculates the possibilities of switching the dynamics from chaotic to periodic by a parameter variation. The measure is applied right away to our model and two useful sets for attaining suppression are computed. In Sec. V, a method to eliminate high fractality from chaotic parameter sets is tested in a system consisting of ten globally coupled Hénon maps, for which it has been proved that very interspersed regions of chaotic and periodic behavior exist.[12] Finally, Sec. VI is devoted to conclusions and discussion.

II. MODEL DESCRIPTION

Nonfeedback methods have been mainly used to suppress chaos in periodically driven dynamical systems. Among them, a wide and important class is represented by forced nonlinear oscillators, whose equation of motion may be written as

$$\ddot{x} + \mu\dot{x} + \frac{dV}{dx} = F\sin\omega t. \qquad (1)$$

It is then reasonable to use a system of this kind to develop our new concepts. In particular, we shall utilize the double-well Duffing oscillator, which is a paradigmatic example. This oscillator corresponds to a unit mass particle in a potential of the form $V(x) = -x^2/2 + x^4/4$, with dissipative coefficient μ and an external harmonic periodic driving of amplitude F and frequency ω. Here, we fix $\omega = 1$ for convenience. The equation of motion then reads

$$\ddot{x} + \mu\dot{x} - x + x^3 = F\sin t. \qquad (2)$$

Depending on the values F and μ, this system can exhibit three main kind of asymptotic bounded solutions: equilibria, periodic motion, and chaotic motion. This Duffing oscillator possesses a chaotic attractor when $F = 6.3$ and $\mu = 0.1$, as shown in Fig. 1.

III. CHAOTIC PARAMETER SET

The asymptotic behavior of a dynamical system can be studied by computing the largest Lyapunov exponent, whenever it exists.[13] As is well known, Lyapunov exponents measure the exponential rates of contraction and expansion along the orbits of dynamical systems. Given two available
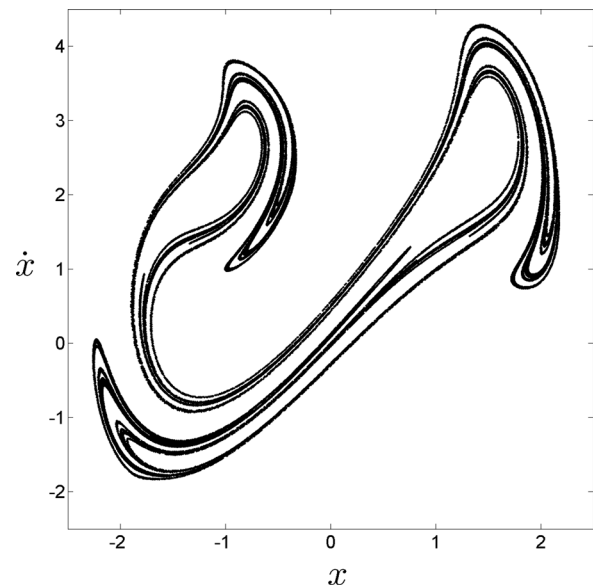

FIG. 1. Chaotic attractor for the Duffing oscillator $\ddot{x} + 0.1\dot{x} - x + x^3 = 6.3\sin t$, with initial conditions $(x, \dot{x}) = (1, 0)$.

parameters of a particular system, the *chaotic parameter set* is defined as the set of the largest Lyapunov exponent computed for every pair of parameter values in a planar grid. This set is a basic and useful tool in the study of dynamical systems[14,15] since it easily allows to visualize the asymptotic behavior of the system in a certain region of the parameter space. We explicitly construct it for the Duffing oscillator to see the procedure. We use the damping coefficient μ and the amplitude of the driving F as the two available parameters of our system, so points in the parameter space are represented by pairs (F, μ). We take a grid of 720×720 points in the rectangle of parameter values $0.02 \leq \mu \leq 1$ and $0 \leq F \leq 15$. For each pair of parameters (F, μ) in the parameter plane the differential equation is solved by means of a fourth order Runge-Kutta integrator, using $(x, \dot{x}) = (1, 0)$ as initial condition. The Lyapunov exponent of the corresponding orbit is evaluated by standard methods and then a different color is assigned depending on the sign and value of the Lyapunov exponent. Those points in the (F, μ) plane with a negative Lyapunov exponent are colored in gray scale, while those with a positive Lyapunov exponent are represented in a nongray colored scale. The resulting plot displays information about the parameter regions with periodic or nonperiodic behavior.

From Fig. 2, it can be inferred that there is a gray scaled "periodic sea" with colored "chaotic islands" in it, similar to the ones described in Refs. 16 and 17. Most of the chaotic islands show striations corresponding to windows of periodicity inside them. Note that by fixing one of the two parameters and varying the other, i.e., by moving along a line parallel to a particular axis in the parameter space, a sort of bifurcation diagram is obtained. Other typical periodic structures that appear are "periodic lakes" connected by "periodic channels." "Periodic lakes" are described and analyzed in the context of high-dimensional chaotic systems in Ref. 10. In particular, "shrimps" are present. These "periodic lakes" are formed by a central elongated body from which narrow
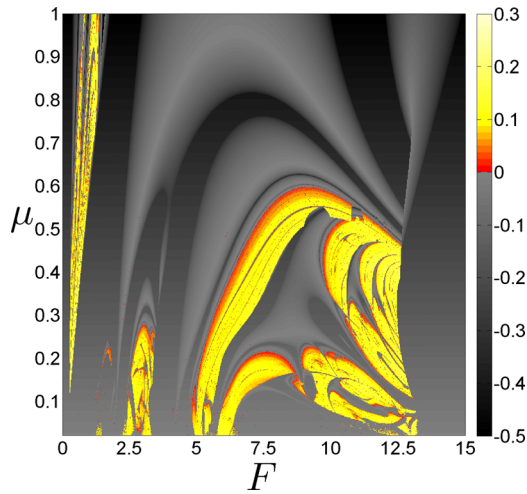
FIG. 2. Chaotic parameter set for the Duffing oscillator $\ddot{x} + \mu\dot{x} - x + x^3$ = $F\sin t$ in the (F, μ) parameter space. The color bar shows the value of the largest Lyapunov exponent, computed for a grid of 720×720 points, and using as initial condition $(x, \dot{x}) = (1, 0)$. Both periodic (gray colored) and chaotic (non-gray colored) motions are displayed.

"periodic channels" come out, resembling shrimp pleopods. Their structure and fractal distribution in parameter space are thoroughly inspected in Ref. 18. Unless a dynamical system exhibits robust chaos,[19] what means that a chaotic regime is preserved by small variations of the parameters and the initial conditions, chaotic regions will generally present fractally distributed "periodic lakes" inside them.[14,15] Similarly, in bifurcation diagrams of non robust systems, such us the logistic map, periodic windows densely fill chaotic regions, lending such diagrams their fractal nature.

IV. EFFECTIVE SUPPRESSIBILITY OF CHAOS

The main purpose of this paper is to define a measure that allows us to quantify the possibilities of effectively suppressing the chaotic dynamics of a system. To this end, we make use of the chaotic parameter set. Nevertheless, this set is a delicate tool for several reasons. The most remarkable one is that chaotic parameter sets usually display fractal structure, so that chaotic regions hide "periodic lakes" inside them at any scale. Moreover, in some sort of systems, even periodic regions reveal chaotic states at any scale as one zooms in. Attending more general considerations, the function we are about to define is resolution dependent. High resolutions are required to make this new tool useful. We always use for convenience a resolution $R \times R$ in the calculations of all our chaotic parameter sets of 720×720. Concerning initial conditions, we suppose they are somehow accessible to suppress chaos. In the worst case, it would be desirable that the chaotic attractor passed close to the point in the phase space corresponding to such initial conditions. These are major restrictions but will always be present whenever we make use of bifurcation diagrams and chaotic parameter sets as guides to suppress chaos.

The basic idea of suppression is to vary a free parameter, the *suppressing parameter*, from a particular value for which chaos rules, to another value for which periodic regime exists. Since we are only interested in the sign of the largest

Lyapunov exponent, we represent chaotic parameter sets as binary sets, assigning black color to chaos and white to periodic dynamics. In this manner, we have an $R \times R$ matrix of grid points, and black or white squares centered in them. For convenience, we identify the square and its centre and simply refer to it as a pixel. Each of these pixels (i, j) is related to a point in the parameter space (F_i, μ_j), with $i, j = 1, \dots, R$. Chaos suppression in the chaotic parameter set simply corresponds to a *transition* from a black pixel to a white one, both contained in a line parallel to the axis associated to the suppressing parameter. We call each of these lines in a chaotic parameter set a *suppressing line* (see Fig. 3). Returning to our model, we take F as the suppressing parameter and fix the value of μ. If there is a particular point in the parameter space (F_i, μ_j) for which chaotic dynamics occurs, we can switch it to periodic by varying the suppressing parameter, i.e., by making a transition to a different point in the same suppressing line (F_k, μ_j). Therefore, pixels in a suppressing line provide a natural way to measure how much a particular chaotic attractor can be suppressed. Simply count all the transitions from that black pixel to all the white ones contained in such line.

At this point, an important objection arises. It could happen that many (possibly infinite) periodic lakes were hidden in that black pixel, allowing transitions to a regular regime by smaller variations of the parameter. This is certainly true, but, in such a case, a smaller region of the chaotic parameter set should be computed. Then the same objection would arise again and again due to the fractal character of the chaotic parameter set. However, even if this was the case, experimentally there is a limitation on the measurement of the suppressing parameter F, imposed by the experimental uncertainty ΔF. This implies a restriction in the range of
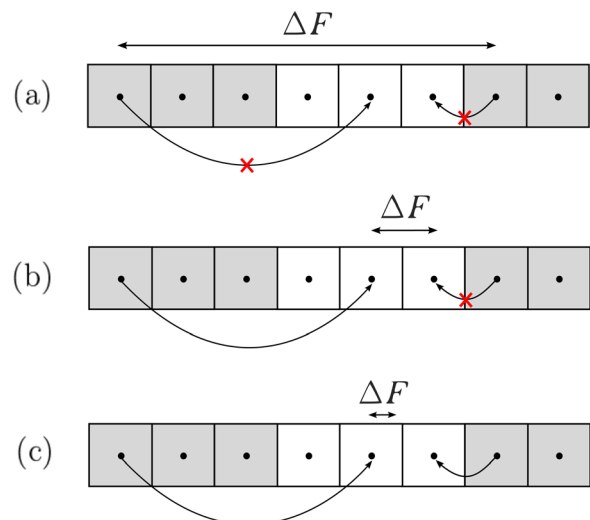

FIG. 3. (a) A suppressing line of eight pixels with an uncertainty ΔF in the measurement of the suppressing parameter F of seven pixels. Two unsafe transitions are shown among all the possible. In this case, no matter which black pixel we are in, no transition to any white pixel guarantees suppression, since the distance to the closest black pixel is always smaller than the uncertainty. (b) Same suppressing line with an uncertainty of one pixel. Now only transitions to white pixels one pixel away from any black one are unsafe. (c) The suppressing line with an uncertainty of a little less than half a pixel, for which all transitions are safe.
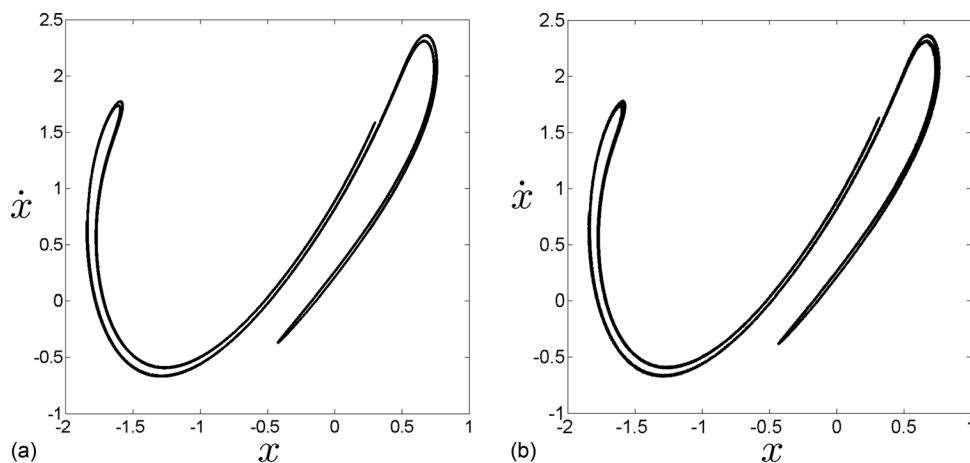
FIG. 4. (a) Chaotic attractor for the Duffing oscillator $\ddot{x} + 0.34\dot{x} - x + x^3 = 6.8 \sin t$. (b) Same chaotic attractor, though letting the driving amplitude fluctuate randomly in the interval [6.76, 6.84], what corresponds to an uncertainty $\Delta F = 0.04$. This attractor looks a bit thicker, but preserves the shape.

values of the suppressing parameter used to compute the chaotic parameter set. The reason is that if a white pixel is at a distance from a black one smaller than the uncertainty, suppression cannot be guaranteed by a transition to that pixel. We define transitions that do not assure suppression as *unsafe transitions*. On the contrary, those that guarantee suppression are named *safe transitions*. Pixels involved in safe (unsafe) transitions are referred as safe (unsafe) too. We also define the length of a suppressing line L as the distance used to compute the chaotic parameter set in the suppressing direction. In the example shown in Fig. 2 this length corresponds to the width of the chaotic parameter set $L = |F_{max} - F_{min}| = 15$. This width must be chosen according to the uncertainty in the measurement of the suppressing parameter. In particular, it must never be smaller than the uncertainty, because in that case we would not be able to guarantee suppression by any specific transition. In other words, all transitions would be unsafe, as is shown in Fig. 3(a). Even more, it is convenient that the uncertainty of the suppressing parameter be much smaller than the length of the suppressing lines. For instance, an adequate length could be such that we assign an uncertainty ΔF of one pixel. This means $\Delta F = L/R$. If this is the case, only transitions to white pixels one pixel away from black ones would be unsafe, as we show in Fig. 3(b). Concerning uncertainty, all the transitions can be considered as safe for $\Delta F < L/2R$, as Fig. 3(c) shows.

Once the chaotic parameter set has been computed taking into account the preceding considerations, black pixels will be taken as chaotic no matter if periodic lakes are hidden inside them. This is a reasonable assumption, since not only periodic regions are hidden by a black pixel but also chaotic ones must be hidden as well. If chaos did not occur experimentally by setting the parameter values to the ones corresponding to that black pixel, an arbitrary small deviation from that value would yield a chaotic motion. Even more, recall that the uncertainty generally comes from two different sources, namely, measuring tools and noise. If fluctuations due to the later are significant compared to the former, chaotic motion will be followed in the black pixel. The reason is that, even if a periodic window is found for some time in that black pixel, for fast enough fluctuations, the system can be expected not to spend long times inside this window,

and rather chaotic motion appears. As an example, consider a chaotic attractor associated to a black pixel centered in $(F, \mu) = (6.8, 0.34)$. In Fig. 4, we show that if we suppose a value of the uncertainty $\Delta F = 0.04$ (two pixels, approximately), a similar attractor is obtained. The later is a bit thicker, but the structure is preserved.

On the other hand, we wonder if white pixels can conceal chaotic regions. In such a case, transitions to them would not be safe at all, making suppression uneffective. At first glance, if one has in mind a periodic window in an archetypal bifurcation diagram, as for example, the one corresponding to the logistic map, by zooming in a periodic window, no chaotic regions are found. However, some situations in which this might occur can be pointed out. The most simple case is a pixel, whose center lands on a periodic window, but the rest of it is occupied by chaotic regions, like the one shown in Fig. 5(a). Also in the boundary between white and black regions this might happen, as is the case of the pixel labeled (b) in the same figure. Next paragraph clears out that these circumstances can be avoided by taking a parameter uncertainty of at least one or two pixels. Other less trivial situation is the coexistence of attractors. If one of those attractors happened to be chaotic, the boundary between them would be fractal, so a very small uncertainty in the measurement of the parameter could lead to the chaotic attractor. When computing bifurcation diagrams one tries to avoid this by following attractors. This means that the last point of the trajectory of the system computed for a particular value of the parameter is used as initial condition to compute the trajectory for the next value of the parameter.
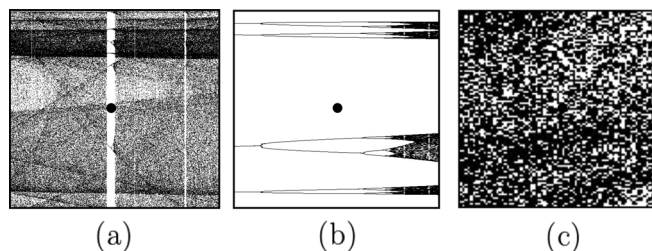

FIG. 5. (a) A white pixel has its center in a periodic window. (b) A white pixel whose center lands in the beginning of a period doubling cascade leading to a chaotic attractor. (c) A zoom in a white pixel containing plenty of black pixels.

With chaotic parameter sets we do not do so. The most dramatic situation happens when there are regions with very interspersed white and black pixels, meaning by very interspersed that white pixels hide black ones at any scale (see Fig. 5(c)). In Sec. V, we provide a method to eliminate these spurious white pixels.

Suppose now we compute a chaotic parameter set with an uncertainty of just one pixel, and we are in a black (chaotic) pixel located at position (i, j). If the first coordinate i corresponds to the suppressing direction and a neighboring pixel $(i\pm 1, j)$ is white, we should not make a transition to it, because it is unsafe. Even worse, we cannot even assure that the first was certainly chaotic. Therefore boundaries in the direction of the suppressing parameter must be redefined by marking as unaccessible all the pixels that are at a distance equivalent to the parameter uncertainty from the boundary. This is explained in Fig. 6 and explicitly done in Fig. 10(a). The remaining pixels in that suppressing line are safe, and so are all the transitions from one of those black pixels to the white ones in the same line. We define all the transitions from a safe black pixel (i, j) to all the safe white ones in a specific suppressing line j as the *set of accessible transitions* $\mathcal{A}_{ij}$ corresponding to that initial chaotic attractor. These transitions are called safe or effective in the sense that for the initial pixel chaos occurs and the final white pixel guarantees suppression.

The distance between two elements involving a transition, or in a similar fashion, how much the parameter must be varied to achieve a certain transition, is also a very important fact when measuring how much can be suppressed the dynamics of a particular black pixel. If we have two possible or accessible transitions, one of them implying a variation of the parameter of two pixels, while another meaning a variation of eight pixels, it seems reasonable to prefer the first one. Hence, the next step is to find a way of considering preferably transitions involving shorter variations of the parameter. The problem is to establish a mechanism to tell how much preferable are short transitions to large ones. Certainly here one has to deal with some arbitrariness, which is going to depend on the conditions we settle to achieve suppression. For instance, we might want to weight very high short transitions and then very low long ones. Or maybe we prefer to weight the same
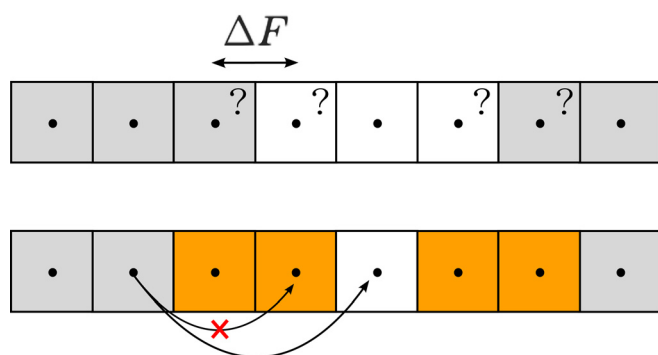

FIG. 6. A suppressing line with unaccessible regions due to precision limitations in the measurement of a parameter denoted by question marks. Pixels at a distance to the boundary smaller than the uncertainty in the measurement of the suppressing parameter ΔF are marked in orange. Transitions involving these pixels are unaccessible.

transitions up to a certain distance and then let their weight decrease slowly, etc. Therefore, given two pixels in a suppressing line, (i, j) and (k, j), we define the *order* of the transition $(i, j) \rightarrow (k, j)$ as the distance between them $|i - k|$, considered as matrix elements in a suppressing line j. Then we assign a *weight* w_{ik} to every transition, through a monotonically decreasing function $w : \mathbb{N} \rightarrow \mathbb{R}$ depending on the order of the transition $w_{ik} = w(|i - k|)$ (see Fig. 8(a)). For example, if we take $w(n) = 1/n$, a black pixel (i, j) and a white pixel (k, j), the transition between them has a weight $w_{ik} = 1/|i - k|$. In this case first order transitions have weight 1, second order transitions have weight 1/2, and, in general, the nth order transition has weight $1/n$. We also require that $w(1) = 1$, what simply gives unit value to the highest possible weight. Finally, we define the suppressibility χ_{ij} on a black pixel (i, j) as the sum of all the weights over the set of accessible transitions $\mathcal{A}_{ij}$, i.e., the weights related to all the safe transitions to white pixels in the same suppressing line

$$\chi_{ij} = \sum_{k \in \mathcal{A}_{ij}} w_{ik}. \tag{3}$$

Now, given two chaotic situations and some particular suppressing conditions coded in w, we can quantitatively compare them to know which one offers more and better possibilities of being suppressed in a certain region of the parameter space. As an example, we consider the two chaotic attractors for parameter choices $(F_{387}, \mu_{132}) = (8.0625, 0.1797)$ and $(F_{555}, \mu_{298}) = (11.5625, 0.4057)$ in Fig. 2. We recall that (F_{387}, μ_{132}) corresponds to the values of the forcing amplitude and damping associated to the grid point given by the coordinates (387, 132) in the computed chaotic parameter set, whose resolution is 720×720. Keep F as the suppressing parameter and suppose it is experimentally measured with a precision $\Delta F = 0.021$, what corresponds to one pixel in the mentioned figure. What is the suppressibility for each of those two attractors if we want to use no more than thirty pixels (variations of the suppressing parameter less or equal than 0.6241) to suppress chaos and consider all transitions equally weighted? These conditions impose an assignment of weights according to a Heaviside function of the form

$$w_{ik} = \begin{cases} 1 & |i - k| \le 30 \\ 0 & |i - k| > 30 \end{cases}. \tag{4}$$

Computation of the suppressibility yields $\chi_{(387,132)} = 8$ and $\chi_{(555,298)} = 7$. This means that under the experimental conditions stated in the previous paragraph, the first attractor offers more possibilities of being suppressed. Now that this is well understood, we define the *suppression parameter set* as the value of the suppressibility computed for every safe black pixel in the chaotic parameter set. This set shows where chaos can be more easily and in more ways suppressed, as shown in Fig. 7. Note that many chaotic attractors have disappeared, since they cannot be suppressed under the specified experimental restrictions imposed by w and ΔF.

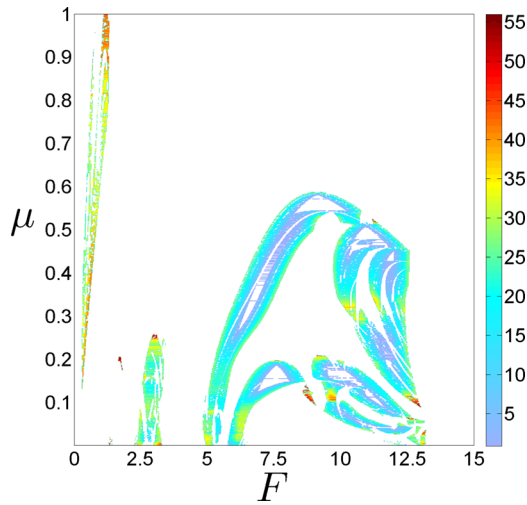Some more information can be extracted from the chaotic parameter set if our function is recast by considering

FIG. 7. Suppression parameter set for $\ddot{x} + \mu\dot{x} - x + x^3 = F\sin t$ in the (F, μ) parameter space, with suppressing parameter F, uncertainty $\Delta F = 0.021$ and $w_{ik} = 1 - \Theta(|i - k| - 30)$, where $\Theta(x)$ is the Heavyside function. This set shows all the safe chaotic events for which chaos can be suppressed, and which ones offer better possibilities of being suppressed, according to the conditions imposed by w. It is obtained by computing the suppressibility χ_{ij} for every safe black pixels (i, j) and assigning each chaotic event a color depending on its value. The color bar goes from cold colors to hot ones, corresponding, respectively, to the lower (1) and higher (56) values of the suppressibility measure.

the accessible transitions from every safe black pixel in a suppressing line. For this reason, we define the *set of the total accessible transitions* $\mathcal{A}_j$ in a suppressing line j as

$$\mathcal{A}_j = \bigcup_{i=1}^{R} \mathcal{A}_{ij}. \tag{5}$$

Note that if the pixel (i, j) is white, $\mathcal{A}_{ij} = \varnothing$, for the only reason that there is no chaos to suppress. This leads to the definition of the *total suppressibility* χ_j for every suppressing line j as the sum of the suppressibility over all the chaotic attractors. This allows us to compare the possibilities of suppressing dynamics via variations of F for different values of the remaining parameter μ appearing in the chaotic parameter set. The new function reads
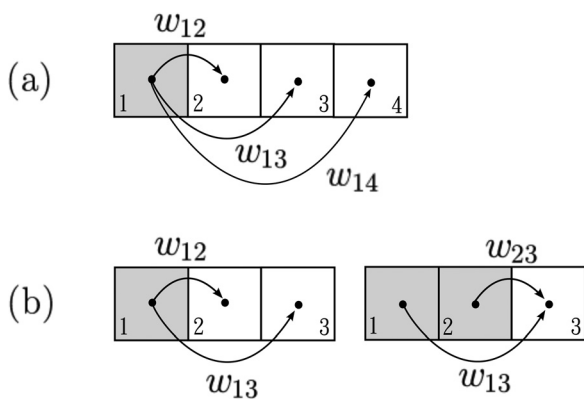

FIG. 8. (a) First, second, and third order transitions in a suppressing line. Since longer transitions contribute less or equal than shorter ones, we have $w_{12} \geq w_{13} \geq w_{14}$. This explains the monotonic decreasing character of w. (b) Two suppressing lines having the same total suppressibility but different number of black pixels or chaoticity. Note that $w_{12} = w_{23} = 1$.

$$\chi_j = \sum_{i,k \in \mathcal{A}_j} w_{ik}. \tag{6}$$

The problem that arises by doing this is that we get a symmetry. For instance, in a suppressing line formed by three pixels, the total suppressibility of two transitions starting from a black pixel to two white consecutive pixels weight the same than two transitions from two black consecutive pixels to a third periodic one (see Fig. 8(b)). To avoid this ambiguity, we define the *chaoticity* κ_j of a suppressing line j as the fraction of chaotic events in it. Our pursued final goal is to compute simultaneously the total suppressibility and the chaoticity for every suppressing line. In other words, we want to know the total suppressibility and the chaoticity as a function of the remaining parameter μ. Results are shown in Fig. 9, where the total suppressibility appears in black for all the values of the damping, and the chaoticity is represented in red. Every value of the total suppressibility has been divided by the maximum value it takes over the chaotic parameter set, which occurs approximately for $\mu = 0.155$.

Note that, on average, the total suppressibility resembles chaoticity in this example. The reason is quite obvious, since starting from a low number of black pixels, the more chaotic events, the more can be suppressed. However, there is a tacit compromise between the number of chaotic and periodic events. If there are too many black pixels along a suppressing line, then there are few white ones to achieve suppression, just the same way that if there are few chaotic events, little chaos can be suppressed.

A distribution with half of the pixels being black and the other half being white (chaoticity $\kappa = 0.5$) would be the optimum situation. On the other hand, for a fixed number of black pixels, the more spread chaotic islands are over the
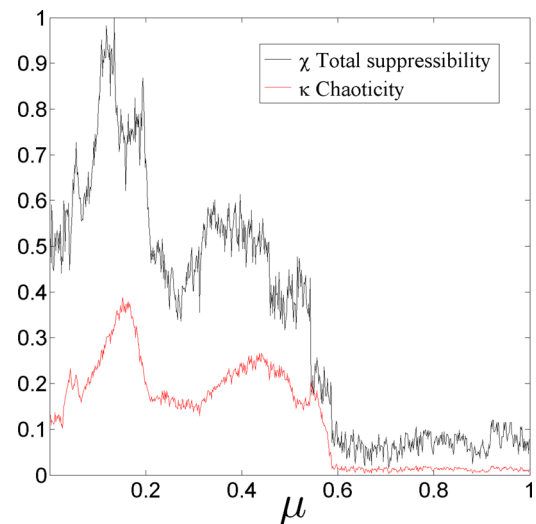

FIG. 9. A plot of the total suppressibility χ (black line) together with chaoticity κ (red line). The former reaches its maximum for $\mu = 0.155$, where chaos is better spread. The more alternation of chaotic and periodic events there is, the higher the total suppressibility. This implies that the closer the chaoticity is to 0.5, the higher the total suppressibility. In this case, chaoticity reaches a maximum close to 0.4, near the value of the damping for which the maximum total suppressibility is obtained. For very high values of the damping, mainly periodic events appear, so there is little chaos to be suppressed and either χ or κ take low values.
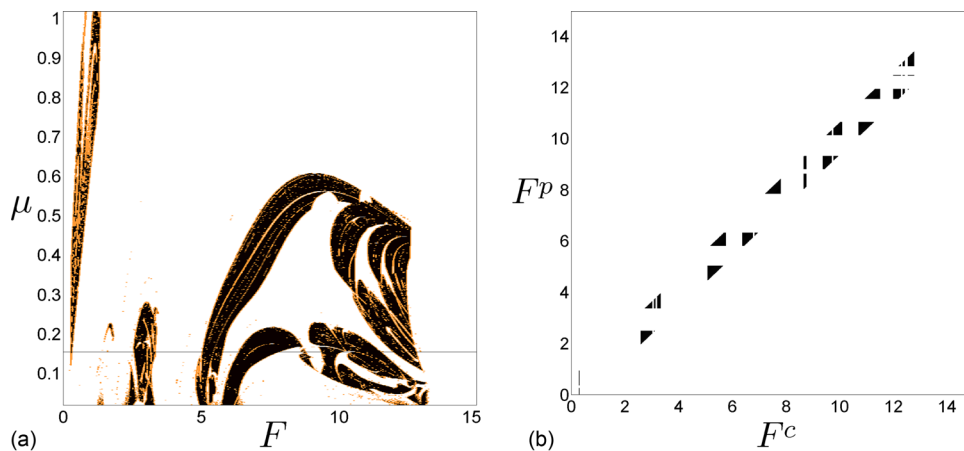
(a)

(b)

FIG. 10. (a) Chaotic parameter set for $\ddot{x} + \mu\dot{x} - x + x^3 = F\sin t$ in the (F, μ) parameter space with suppressing parameter F, uncertainty $\Delta F = 0.021$ and $w_{ik} = 1 - \Theta(|i - k| - 30)$. Unsafe regions due to uncertainty are colored orange. The thin horizontal line represents the value of the damping $\mu_{144} = 0.155$ for which a maximum total suppressibility is obtained. (b) The set of the total accessible transitions $\mathcal{A}_{114}$ for that maximum. The plot displays transitions involving different values of the suppressing parameter F. In the x axis, the values of the forcing for the initial state indicated with the superscript c, while in the y axis the values of the forcing for the final state in the transition, denoted by p. If the starting pixel corresponds to chaotic (c) motion and the transition leads to periodic (p) regime, the point is colored black. Otherwise the transitions are left uncolored. Note the great alternation of white and black.

periodic sea (along a suppressing line), the closer they are from it, so the lower chaos suppressing transitions tend to be. Therefore, two things contribute to an increase of the total suppressibility: an alternance of black and white regions and the equality of chaotic and periodic events. Both together mean that chaos is better spread, so can be more easily suppressed. Also note that the total suppressibility experiences more fluctuations than the chaoticity. In general terms, the suppressibility depends not only on the number of black pixels but also on the suppression conditions coded in w. If large transitions are heavily weighted by this function, then a slight difference of chaotic events can seriously affect the value of the function.

In Fig. 10(a), we show the chaotic parameter set with unsafe chaotic and periodic events colored in orange. The thin straight line represents the value of the damping for which the maximum total suppressibility is obtained. Beside it, in Fig. 10(b), the set of the total accessible transitions for that maximum is shown. The horizontal axis represents the value of the suppressing parameter F for the initial states in that suppressing line. The vertical axis shows all the possible final values. Those transitions $F_i \to F_k$ starting from a chaotic state and leading to periodic motion are marked in black. The reason

why these transitions are contained in a vertical strip around the diagonal is that the chosen w only allows counting up to thirty pixels far form the initial region. Note that the closer we are to the diagonal the shorter the transition is.

V. ELIMINATING SPURIOUS PIXELS

White pixels containing chaotic regions are spurious in the sense that they might not assure suppression of chaos. Therefore, to make suppression effective, they must be eliminated from chaotic parameter sets when studying suppressibility. This phenomenon, the existence of white pixels hiding chaotic motion, might happen for several reasons, and among all its possible manifestations, most distressing examples occur when a white pixel hides chaotic ones at any scale. This strong fractality is far from being a mere curiosity but suggested to be a robust phenomenon for globally coupled systems.[12]

A possible way of measuring the fractality of a set is the *uncertainty exponent* α.[20,21] On the chaotic parameter set, this uncertainty exponent is related to the probability that two parameters, arbitrarily close, yield different asymptotic behavior. The relation is the typical power law, $P(\epsilon) \propto \epsilon^{\alpha}$, where ϵ is the distance between the two parameters. Therefore, the
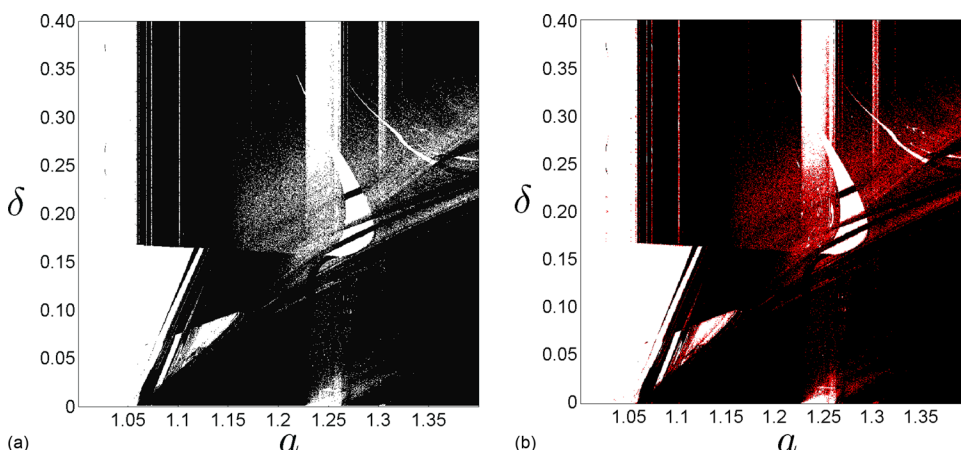

(a)

(b)

FIG. 11. (a) Chaotic parameter set in (a, δ) space for ten globally coupled Hénon maps. Note the dusty regions, where chaotic (black) and periodic (white) asymptotic motion are very interspersed. (b) Same chaotic parameter set after the application of the algorithm. Spurious white pixels are marked in red.
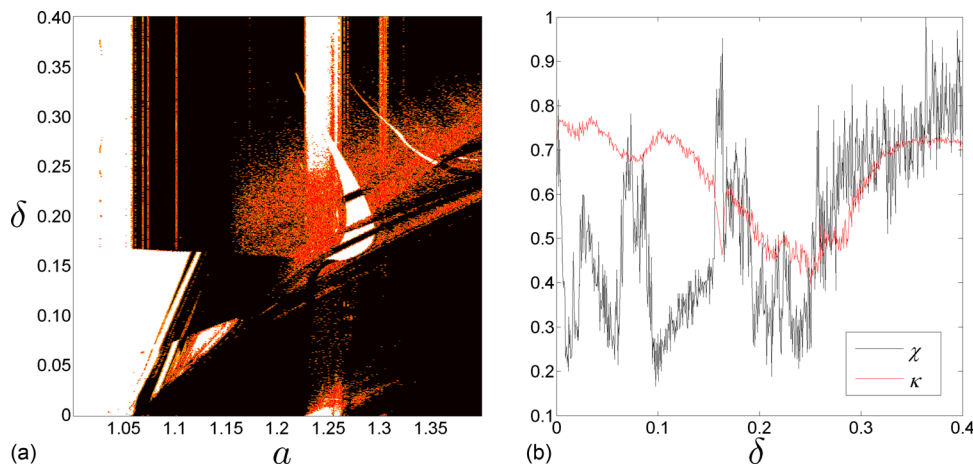
FIG. 12. (a) Cleaned chaotic parameter set in the (a, δ) space for ten globally coupled Hénon maps. Unaccessible regions due to spurious pixels are marked in red, while those due to a lack of precision in the measurement of a parameter are marked in orange. (b) Total suppressibility χ in black together with chaoticity κ in red.

uncertainty exponent measures the relation between the accuracy in the calculation of a parameter and the ability to predict the asymptotic dynamics correctly. If the exponent is too close to zero, it does not matter how much we improve the precision, since we are not capable of predicting the final state. A simple algorithm based on the uncertainty exponent can be developed: for each white pixel calculate the uncertainty exponent and, if its value is smaller than a certain established parameter value, then eliminate it. However, this would be unnecessarily high time consuming. To optimize computational resources, an even simpler algorithm can be performed: for every white pixel in the chaotic parameter set, calculate a high enough number of randomly chosen points of the parameter space. Whenever a positive largest Lyapunov exponent shows up, we mark that pixel as unaccessible.

We shall utilize a similar parameter space than the one presented in Ref. 12, corresponding to ten globally coupled Hénon maps. This sort of systems appears in broad branches of science, since they are approximations of spatiotemporal dynamical systems governed by nonlinear partial differential equations. For a more detailed study of the system we refer to the cited paper. The set of equations governing its dynamics reads

$$x_{n+1}^i = a - \left((1-\delta)x_n^i + \delta/9 \sum_{j \neq i} x_n^j \right)^2 + b y_n^i$$
$$y_{n+1}^i = x_n^i, \tag{7}$$

where $i = 1, \ldots, 10$.

The parameters a and b correspond to the Hénon map and δ is the coupling strength. We use $1.0 \leq a \leq 1.4$ and $0.0 \leq \delta \leq 0.4$ to compute the chaotic parameter set, taking a as the suppressing parameter. The remaining parameter is fixed $b = 0.3$. The chaotic parameter set in (a, δ) is shown in Fig. 11(a), computed for the initial conditions $(x_0^1, y_0^1) = (1, 0)$ and $(x_0^i, y_0^i) = (0, 0)$ for $i \neq 1$. Dusty regions where chaotic and periodic motions are very interspersed occur. In such regions, if one makes a zoom in a white pixel, always black pixels show up, no matter how small the scale is.

The algorithm is operated using twenty random values of a for each white pixel to eliminate spurious cases. Whenever a positive Lyapunov exponent shows up in a white pixel, it is

marked in red, as in Fig. 11(b). Afterwards, we eliminate unsafe regions due to precision limitations, supposing an experimental uncertainty of $\Delta a = 0.00056$, and painting them in orange. Having cleaned up our chaotic parameter set, the total suppressibility is computed. Weights are assigned according to the function $w(n) = e^{(1-n)/10}$, what means that the preference in transitions decays exponentially as the distance grows, with decay constant 10. Results can be observed in Fig. 12.

From a coupling strength, $\delta = 0$ in Eq. (7), the total suppressibility starts decreasing rapidly because the white central region becomes dusty. Then it begins to increase, again as a consequence of the white lakes appearing for $a \approx 1.1$. Suddenly, these regions turn unaccessible and are rapidly recovered. This explains the two first spikes represented in Fig. 12(b). Once this region disappears, the total suppressibility falls to its minimum, for $\delta \approx 0.1$. A black ascending stripe born on the left white region follows allowing new transitions, what explains the positive slope of the curve. Chaoticity does not increase in this step because black pixels are disappearing on the right side of the stripe and also some become unaccessible due to uncertainty (orange) around spurious (red) pixels. When the white curved region resembling a boomerang is born for $a \approx 1.26$, the total suppressibility suddenly jumps to its third highest value. This does not last long, because this region is widely surrounded by unaccessible ones, being the accessible regions very far away, so weighted very little by w, that decay exponentially. This, together with the narrowing of the boomerang, drops the total suppressibility again to low values. Then, it begins to climb towards its maximum as a consequence of the rectangular white region with which the boomerang merges, for high values of δ. Now, the total suppressibility does not resemble the chaoticity. For instance, up to $\delta = 0.3$, the later tends to decrease, while the total suppressibility experiences great oscillations.

VI. CONCLUSIONS AND DISCUSSION

In summary, our investigation provides a precise quantitative method to determine the possibilities of suppressing the chaotic motion of a system by a time independent variation of a parameter. The method is based on the definition of a new measure, the suppressibility, defined in the parameter space. Since it has mainly practical purposes, it depends on

experimental precisions and suppressing conditions. Suppressibility has allowed us to compute the suppression parameter set, which shows a region in parameter space with all the chaotic attractors that can be effectively suppressed, and what possibilities offer to achieve such a suppression. Afterwards, the total suppressibility has been introduced allowing us to compare the possibilities of suppressing chaos throughout different values of another parameter. In this manner, when desiring to suppress chaotic dynamics of a system by varying a certain parameter with less difficulties, we can figure out in what regions of another available parameter is worth working. Having fixed such parameter at an appropriate value, the set of the total accessible transitions has been computed. This set allows to see at a glance the transitions that yield predictable behavior. Finally, since all this work is accomplished in the chaotic parameter set, we have proposed a mechanism to clean it from spurious events, making our technique more effective.

ACKNOWLEDGMENTS

[1] Y. Braiman and I. Goldhirsch, Phys. Lett. **66**, 2545 (1991).
[2] R. Lima and M. Pettini, Phys. Rev. A **41**, 726 (1990).
[3] R. Chacón and J. D. Bejarano, Phys. Lett. **71**, 3103 (1993).
[4] F. Rodelsperger, Y. S. Kivshar, and H. Benner, Phys. Rev. E **51**, 869 (1995).
[5] E. Ott, C. Grebogi, and J. Yorke, Phys. Rev. Lett. **64**, 1196 (1990).
[6] J. M. Seoane, S. Zambrano, S. Euzzor, R. Meucci, F. T. Arecchi, and M. A. Sanjuán, Phys. Rev. E **78**, 016205 (2008).
[7] M. A. F. Sanjuán, Phys. Rev. E **58**, 4377 (1998).
[8] S. Zambrano, E. Allaria, S. Brugioni, I. Leyva, R. Meucci, M. A. F. Sanjuán, and F. T. Arecchi, Chaos **16**, 013111 (2006).
[9] S. Zambrano, J. Seoane, I. M. no, M. A. F. Sanjuán, S. Euzzor, R. Meucci, and F. T. Arecchi, New J. Phys. **10**, 073030 (2008).
[10] E. Barreto, B. R. Hunt, C. Grebogi, and J. Yorke, Phys. Lett. **78**, 4561 (1997).
[11] L. Fronzoni, M. Giocondo, and M. Pettini, Phys. Rev. A **43**, 6483 (1991).
[12] Y. Lai and R. L. Winslow, Phys. Lett. **72**, 1640 (1994).
[13] W. Ott and J. A. Yorke, Phys. Rev. E **78**, 056203 (2008).
[14] M. P. Dafilis, D. T. J. Liley, and P. J. Cadusch, Chaos **11**, 474 (2001).
[15] H. A. Albuquerque, R. M. Rubinger, and P. C. Rech, Phys. Lett. A **372**, 4793 (2008).
[16] A. R. Zeni and J. A. Gallas, Physica D **89**, 71 (1995).
[17] J. Gallas, Appl. Phys. B: Lasers Opt. **60**, S203 (1995).
[18] J. A. C. Gallas, Phys. Lett. **70**, 2714 (1993).
[19] S. Banerjee, J. A. Yorke, and C. Grebogi, Phys. Rev. Lett. **80**, 3049 (1998).
[20] C. Grebogi, S. W. McDonald, E. Ott, and J. A. Yorke, Phys. Lett. A **99**, 415 (1983).
[21] J. Aguirre, R. Viana, and M. A. F. Sanjuán, Rev. Mod. Phys. **81**, 333 (2009).